IEEE Photonics Journal
An IEEE Photonics Society Publication

Photonic Microwave Up-Conversion Link With Compensation of Chromatic Dispersion-Induced Power Fading

Volume 11, Number 4, August 2019

Dan Chen
Tao Shang
Xiongchao Liu
Gufeng Li
Yinling Zhang

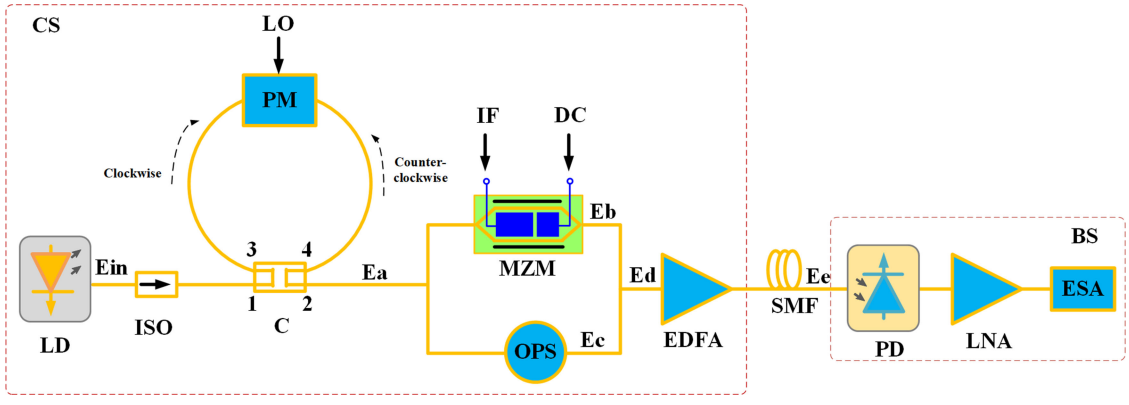

DOI: 10.1109/JPHOT.2019.2928031

Photonic Microwave Up-Conversion Link With Compensation of Chromatic Dispersion-Induced Power Fading

Dan Chen,[1,2] **Tao Shang**,[1,2] **Xiongchao Liu**,[1,2] **Gufeng Li**,[1,2] **and Yinling Zhang**[1,2]

[1]State Key Laboratory of Integrated Service Networks, School of Telecommunications Engineering, Xidian University, Xi'an 710071, China
[2]Collaborative Innovation Center of Information Sensing and Understanding, Xidian University, Xi'an 710071, China

DOI:10.1109/JPHOT.2019.2928031

Manuscript received May 16, 2019; revised June 19, 2019; accepted July 8, 2019. Date of publication July 12, 2019; date of current version July 26, 2019. This work was supported in part by the 863 High Technology Plan of China under Grant 2013AA013402, and in part by the National Natural Science Foundation of China under Grants 61172080, 61771357, and 61805189. Corresponding author: Dan Chen (email: danchen_zx@163.com).

Abstract: An effective scheme of frequency doubling up-conversion is proposed and demonstrated, which achieves the generation of high-frequency microwave signal and the compensation of chromatic dispersion-induced power fading (CDIPF). The system structure is based on a cascading of a Sagnac loop and a Mach–Zehnder modulator (MZM), where a phase modulator is used in the Sagnac loop. In the loop, only the clockwise propagating light wave is modulated by a small local oscillator signal, leaving the counter-clockwise propagating light wave unmodulated because of the velocity mismatch. The output signal is divided into two parts, one traveling into an MZM and the other entering an optical phase shifter. The intermediate frequency signal is supplied to the MZM, which is biased at its minimum point and then the carrier-suppressed double sideband is achieved. With the adjustment of the optical phase shift, the CDIPF can be compensated at any frequency. In the simulation, by comparing the frequency responses of the proposed link with and without dispersion compensation, we successfully demonstrate the performance of power fading compensation for 60- and 80-km link. Consequently, the spurious-free dynamic range is effectively improved by 13.54 dB at 22.6 GHz for 60-km link.

Index Terms: Radio over fiber (RoF), up-conversion, power fading, compensation.

1. Introduction

With the increasing bandwidth requirements of the next generation wireless communication networks [1]–[3], radio over fiber (RoF) technology is regarded as one of the most promising techniques for wideband and multiservice applications, because of some of its inherent advantages, including large signal bandwidth, low link loss and immunity to electromagnetic interference. In the current wireless communication systems, the generation of the high frequency microwave signals and chromatic dispersion compensation of long-distance optical fibers are regarded as the main research directions to achieve the rapid development of RoF links. For high frequency signal applications, the modulation of the RoF links is limited by the modulation bandwidths of the external modulators and LDs, so frequency multiplication up-conversion approach becomes a potential development direction. There are some up-conversion approaches using low bandwidth devices. For example,

the microwave signals are generated using the nonlinearity of the modulators [4], [5]. In [6], the microwave mixing signal is generated by a dual-parallel MZM (DPMZM). One sub-modulator which is biased at the maximum transmission point is driven by a local oscillator (LO) signal in order to suppress the odd-order sidebands. The same case applied to the other sub-modulator with respect to the radio frequency (RF) signal. The scheme can achieve up-conversion with a high conversion gain by properly adjusting the main direct current (DC) bias voltage of the DPMZM.

However, with the development of communication systems and increasing of microwave signal frequency, the chromatic dispersion-induced power fading (CDIPF) becomes a significant limitation factor for the quality of signal transmission. Due to the double sideband (DSB) modulation and power fading effect, the power of the received up-converted microwave signal displays a sine-like fluctuation. Hence, the transmission distance of the link will be eventually limited [7]. In order to overcome CDIPF effect, one effective approach is to use optical single sideband (OSSB) modulation links. Such as, a dual-electrode MZM (DEMZM) which is biased at the quadrature transmission point [8] is used to generate the OSSB signals. In [9], the cascaded polarization modulators (PolMs) are used to generate the OSSB signals and optical carrier-to-sideband ratio can be tuned by adjusting the polarization angle between the light wave and the polarizer.

The other approach to overcome the CDIPF is to use the pre-distorted or post-compensated optical DSB modulation links. In [10], a microwave photonic mixing link based on a dual-drive dual-parallel MZM (DD-DPMZM) is achieved. By adjusting the main DC bias voltage, the microwave signal generation of high conversion efficiency and compensation of the CDIPF can be achieved. In [11], two low-bandwidth MZMs are used to generate an up-converted signal with high dispersion tolerance. And in [12], an up-convertor based on cascaded MZM and DPMZM is implemented. The LO signal is supplied to the MZM which is biased at the minimum transmission point to generate the carrier-suppressed double-sideband (CS-DSB) modulation signal. The two ports of the DPMZM are connected with intermediate frequency (IF) and DC signal sources, respectively. With the adjustment of main DC bias of the DPMZM, the power fading of the link can be compensated. However, these schemes need control of more than one DC bias, which makes the link much more unstable. And if automatic bias controllers are used to mitigate the instability, the system costs will be increased.

Meanwhile, the Sagnac loop has been widely studied for the purposes of dispersion compensation. For example, in [13], the Sagnac loop is used to realize the conversion of phase modulation to intensity modulation (PM-IM), and the frequency response can be adjusted by tuning polarization controller (PC). However, the structure only achieves dispersion compensation without the generation of high frequency microwave signal. In [14], although high frequency microwave signal generation is achieved, the frequency requirement for the LO signal is relatively high. In [15], a phase modulator (PM) in the Sagnac loop is used, and the optical carrier is suppressed with the adjustment of PC. Then, a frequency-doubled signal is generated. However, the change of the polarization state of the system will affect the stability of the system.

In this paper, a novel photonic microwave signal up-conversion scheme with the compensation of CDIPF is proposed. In our proposed system, a small amplitude LO signal is supplied to a PM to realize the CS-DSB modulation. Meanwhile, the LO modulation signal serving as the optical carrier is injected into MZM driven by an IF signal. By adjusting bias voltage of the MZM, the CS-DSB is achieved and only the odd-order sidebands are preserved. Then by appropriately adjusting the phase shift of optical phase shifter (OPS), a high frequency RF signal with compensation of CDIPF is generated at any frequency. Because the LO signal frequency is only one-half of the RF signal frequency, the bandwidth requirement of the modulator is reduced in our proposed scheme. Furthermore, less DC bias control is required compared with [11], [12].

The remainder of this paper is summarized below. In Section 2, the scheme is set up and operational principle is analyzed. In Section 3, we simulate the frequency responses and SFDR of the system, and the simulation results agree well with the theory analysis. Meanwhile, the influence of OPS phase deviation angle and the power distribution imbalance of the power splitter on system performance are verified. Lastly, the conclusion appears in Section 4.

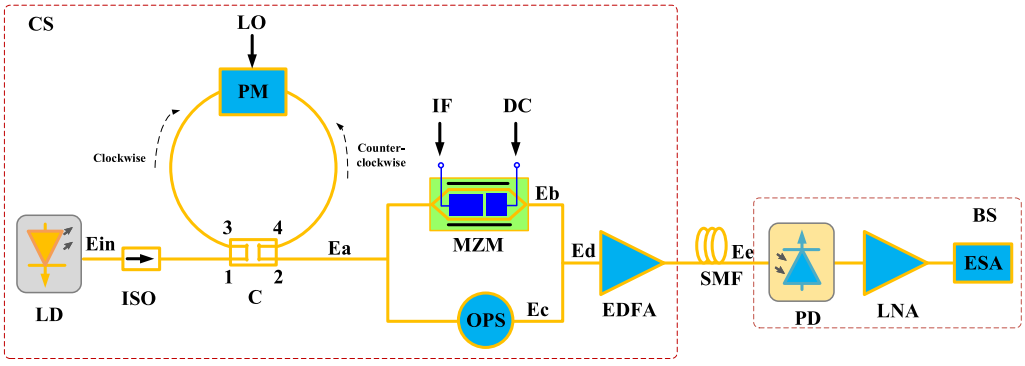

Fig. 1. Schematic diagram of the proposed up-conversion link. ISO: optical isolator; OPS: optical phase shifter; LNA: low noise amplifier; ESA: electric spectrum analyzer.

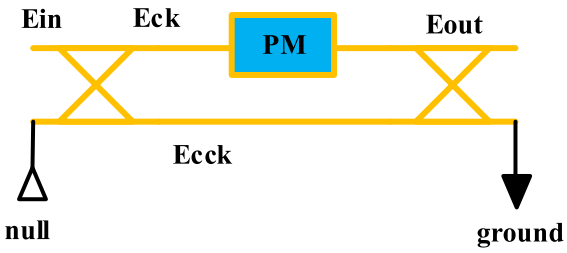

Fig. 2. The structure of the Sagnac loop.

2. Operational Principle

The schematic diagram of the frequency up-conversion and dispersion compensation RoF link in this paper is shown in Fig. 1.

As shown in Fig. 1, in the central station (CS), the proposed link is mainly composed of a laser diode (LD), an optical isolator (ISO), a Sagnac loop, a PM, a MZM, an OPS and an erbium-doped optical fiber amplifier (EDFA). A continuous light wave from the LD is sent to the Sagnac loop via ISO. $E_{in}(t)$ represents the output optical carrier signal of the LD, whose optical field can be represented as $E_{in}(t) = E_0 \exp(j\omega_c t)$. E_o and ω_c are the amplitude and angular frequency of the optical carrier signal, respectively. The Sagnac loop contains two couplers and a PM, and its structure is shown in Fig. 2. For the Sagnac loop [16], [17], the transmission function of the coupler can be given by

$$\begin{bmatrix} E_{out1} \\ E_{out2} \end{bmatrix} = \frac{1}{\sqrt{2}} \begin{bmatrix} 1 & j \\ j & 1 \end{bmatrix} \bullet \begin{bmatrix} E_{in1} \\ E_{in2} \end{bmatrix} \tag{1}$$

So when optical carrier is sent to the first coupler, the clockwise (CK) light wave and the counter-clockwise (CCK) light wave can be written as

$$\begin{bmatrix} E_{CK} \\ E_{CCK} \end{bmatrix} = \frac{1}{\sqrt{2}} \begin{bmatrix} 1 & j \\ j & 1 \end{bmatrix} \bullet \begin{bmatrix} E_{in} \\ 0 \end{bmatrix} = \frac{1}{\sqrt{2}} \begin{bmatrix} E_{in} \\ jE_{in} \end{bmatrix} \tag{2}$$

Because the PM is a traveling-wave modulator, in the CK direction, the LO signal with amplitude of V_{LO} and angular frequency of ω_{LO} is modulated onto the optical carrier. While in the CCK direction, the optical carrier cannot be modulated because of the velocity mismatch between the LO signal and the optical carrier [13]–[15]. After the two optical signals pass through the PM, the modulated

optical signals are written as

$$E_{CKM} = E_{CK} e^{jm_{LO}\cos\omega_{LO}t} = \frac{1}{\sqrt{2}} E_{in} e^{jm_{LO}\cos\omega_{LO}t} = \frac{1}{\sqrt{2}} E_0 e^{j\omega_0 t} e^{jm_{LO}\cos\omega_{LO}t} \tag{3}$$

$$E_{CCKM} = E_{CCK} = \frac{j}{\sqrt{2}} E_{in} = \frac{j}{\sqrt{2}} E_0 e^{j\omega_0 t} \tag{4}$$

where E_{CKM} and E_{CCKM} are the optical field expression of the CK optical signal at the port4 and the CCK optical signal at the port3 of the coupler, respectively. The electro-optical modulation index of the PM is defined as $m_{LO} = \pi V_{LO}/V_{\pi 1}$ and $V_{\pi 1}$ is the half-wave voltage of the PM.

Then the modulated optical signals are combined by the second coupler, and we can obtain

$$\begin{bmatrix} E_a \\ E_{ground} \end{bmatrix} = \frac{1}{\sqrt{2}} \begin{bmatrix} 1 & j \\ j & 1 \end{bmatrix} \bullet \begin{bmatrix} E_{CKM} \\ E_{CCKM} \end{bmatrix} \tag{5}$$

where E_a and E_{ground} are the output signals of the second coupler. E_{ground} is grounded and E_a is the output signal of the Sagnac loop which is expressed as

$$E_a = \frac{1}{\sqrt{2}} (E_{CKM} + jE_{CCKM}) = \frac{1}{2} E_0 e^{j\omega_0 t} (e^{jm_{LO}\cos\omega_{LO}t} - 1) \tag{6}$$

In the case of small signal approximation, only the $\pm$1st order modulation optical sidebands of the LO signal are considered and the other high order sidebands can be neglected. By using Bessel series expansion, equation (6) can be further approximated as

$$\begin{aligned} E_a &= \frac{1}{2} E_0 e^{j\omega_0 t} (j^n J_n(m_{LO}) e^{jn\omega_{LO}t} - 1) \\ &\approx \frac{1}{2} E_0 e^{j\omega_0 t} (J_0(m_{LO}) + jJ_1(m_{LO}) e^{j\omega_{LO}t} + j^{-1} J_{-1}(m_{LO}) e^{-j\omega_{LO}t} - 1) \\ &\approx \frac{1}{2} E_0 e^{j\omega_0 t} (jJ_1(m_{LO}) e^{j\omega_{LO}t} + jJ_1(m_{LO}) e^{-j\omega_{LO}t}) \end{aligned} \tag{7}$$

As we can see from equation (7), CS-DSB modulation signal is obtained. Then the modulated optical signal is divided into two equal parts by a general optical power splitter. One part is sent to a MZM as optical carrier and is modulated by IF signal. The MZM is biased at the minimum transmission point to suppress optical carrier. The other part is sent to an OPS to introduce an additional phase shift φ. Equations (8) and (9) represent the output optical signals of MZM and OPS, respectively.

$$E_b = \frac{E_a}{\sqrt{2}} (e^{j\frac{\pi}{2}} e^{jm_{IF}\cos\omega_{IF}t} + e^{-j\frac{\pi}{2}} e^{jm_{IF}\cos\omega_{IF}t}) \approx (-2)\frac{E_a}{\sqrt{2}} J_1(m_{IF})(e^{j\omega_{IF}t} + e^{-j\omega_{IF}t}) \tag{8}$$

$$E_c = \frac{E_a}{\sqrt{2}} e^{j\varphi} \tag{9}$$

where $m_{IF} = \pi V_{IF}/V_{\pi 2}$ is the electro-optical modulation index of the MZM with half-wave voltage of $V_{\pi 2}$. V_{IF} and ω_{IF} represent the amplitude and angular frequency of the IF signal, respectively.

Then the two parts of the optical signal are combined again through an optical power combiner. The output optical signal of the optical power combiner is expressed as

$$E_d = \frac{E_b + E_c}{\sqrt{2}} = \frac{E_a}{2} \left[(-2) J_1(m_{IF})(e^{j\omega_{IF}t} + e^{-j\omega_{IF}t}) + e^{j\varphi} \right] \tag{10}$$

When we substitute equations (7) (8) (9) into (10), equation (10) can be further expressed as

$$\begin{aligned} E_d = &-\frac{E_0}{2} j e^{j\omega_0 t} J_1(m_{IF}) [e^{j(\omega_{LO}+\omega_{IF})t} + e^{j(\omega_{LO}-\omega_{IF})t} + e^{-j(\omega_{LO}-\omega_{IF})t} + e^{-j(\omega_{LO}+\omega_{IF})t}] \\ &+ \frac{E_0}{4} j e^{j\omega_0 t} J_1(m_{LO}) e^{j\varphi} (e^{j\omega_{LO}t} + e^{-j\omega_{LO}t}) \end{aligned} \tag{11}$$

Next, the output signal is sent to a signal mode fiber (SMF), and the optical field representation of output signal of the SMF is

$$E_e = -\frac{E_0}{2} j e^{j\omega_0 t} J_1(m_{IF}) \left[\begin{array}{l} e^{j(\omega_{LO}+\omega_{IF})t} e^{j\varphi_1} + e^{j(\omega_{LO}-\omega_{IF})t} e^{j\varphi_2} \\ \quad + e^{-j(\omega_{LO}-\omega_{IF})t} e^{j\varphi_2} + e^{-j(\omega_{LO}+\omega_{IF})t} e^{j\varphi_1} \end{array} \right] + \frac{E_0}{4} j e^{j\omega_0 t} J_1(m_{LO}) e^{j\varphi} (e^{j\omega_{LO} t} + e^{-j\omega_{LO} t}) e^{j\varphi_0} \tag{12}$$

where $\varphi_0 = 1/2\beta_2 L\,\omega_{LO}^2$, $\varphi_1 = 1/2\beta_2 L\,(\omega_{LO}+\omega_{IF})^2$, $\varphi_2 = 1/2\beta_2 L\,(\omega_{LO}-\omega_{IF})^2$ are the phase shifts introduced by fiber dispersion and $\beta_2 = -2\pi c D/\omega_0^2$. D, β_2 and L represent dispersion parameter, dispersion coefficient and fiber length, respectively.

For the sake of simplicity, only the ±1st order optical sidebands are considered. After PD, the optical signal is converted into the electrical signal. In order to obtain the signal at the frequency of $2\omega_{LO}+\omega_{IF}$, a filter is used to filter out the components of other frequencies, such as $2\omega_{LO}-\omega_{IF}$. The photocurrent at the frequency of $2\omega_{LO}+\omega_{IF}$ can be written as

$$i(t) \propto E_e E_e^* \propto -\frac{E^2}{8} J_1^2(m_{LO}) J_1(m_{IF}) \left[\begin{array}{l} 2e^{j(2\omega_{LO}+\omega_{IF})t} \cos(\varphi_1 - \varphi_0 - \varphi) \\ +2e^{-j(2\omega_{LO}+\omega_{IF})t} \cos(\varphi_1 - \varphi_0 - \varphi) \end{array} \right]$$
$$= -\frac{1}{2} E^2 J_1^2(m_{LO}) J_1(m_{IF}) \cos(2\omega_{LO}+\omega_{IF}) \cos(\varphi_1 - \varphi_0 - \varphi) \tag{13}$$

As can be seen from the above equation, the up-converted RF signal with angular frequency of $\omega_{RF} = 2\omega_{LO}+\omega_{IF}$ is generated. The photocurrent of the desired RF signal is proportional to $\cos(\varphi_1 - \varphi_0 - \varphi) = \cos\{\beta_2 L\,[(\omega_{LO}+\omega_{IF})^2 - \omega_{LO}^2]/2 - \varphi\}$. In general, the RF photocurrent generated in the traditional frequency doubling up-conversion analog optical link is proportional to the equation $\rho = \cos\beta_2 L\,[(\omega_{LO}+\omega_{IF})^2 - \omega_{LO}^2]/2$. When the LO signal and IF signal are fixed, the photocurrent of the obtained RF signal will periodically change with the transmission distance L. Meanwhile, there will be no way to compensate it. And the maximum power fading and the minimum link gain will be achieved if ρ is set to 0. However, in our proposed link, the optical phase shift φ can be properly adjusted to satisfy equation (14) and then the obtained RF signal photocurrent will be proportional to $E^2 J_1^2(m_{LO}) J_1(m_{IF})$. So the obtained RF signal will not be influenced by CDIPF. That is to say, by adjusting phase shift φ of the OPS to satisfy equation (14), the corresponding dispersion compensation is achieved.

$$\beta_2 L \left[(\omega_{LO}+\omega_{IF})^2 - \omega_{LO}^2 \right] \Big/ 2 - \varphi = k\pi, \quad k \in z \tag{14}$$

After the power compensation, we can realize a larger conversion gain. The photocurrent of RF signal at the frequency of $2\omega_{LO}+\omega_{IF}$ can be given by

$$i(t) \propto -\frac{1}{2} E^2 J_1^2(m_{LO}) J_1(m_{IF}) \cos(2\omega_{LO}+\omega_{IF}) \tag{15}$$

Fig. 3 explains the generation of microwave signal and compensation of CDIPF in the conventional and the proposed frequency up-conversion links. In the conventional link, the optical spectrum before the fiber transmission is shown in Fig. 3(a). The sidebands of LO and IF signals have the same phase. As shown in Fig. 3(b), after the transmission of SMF, the sidebands of LO and IF signals will produce different phase shifts which are φ_0 and φ_1 (or φ_2), respectively. As a result, a destructive interference and power fading will occur on the obtained RF signal after photodetection in Fig. 3(c). However, in our proposed scheme, an additional phase shift φ is added to the LO sidebands before the fiber transmission by adjusting OPS appropriately in Fig. 3(d). The optical spectrum after fiber transmission is shown in Fig. 3(e), where the phase of the LO sidebands is $\varphi_0+\varphi$, while the phase of the IF sidebands will be the same as the conventional link. By adjusting the optical phase shift of OPS, equation (14) is satisfied. The corresponding RF power fading is canceled, which can be found by comparing Fig. 3(c) with Fig. 3(f).

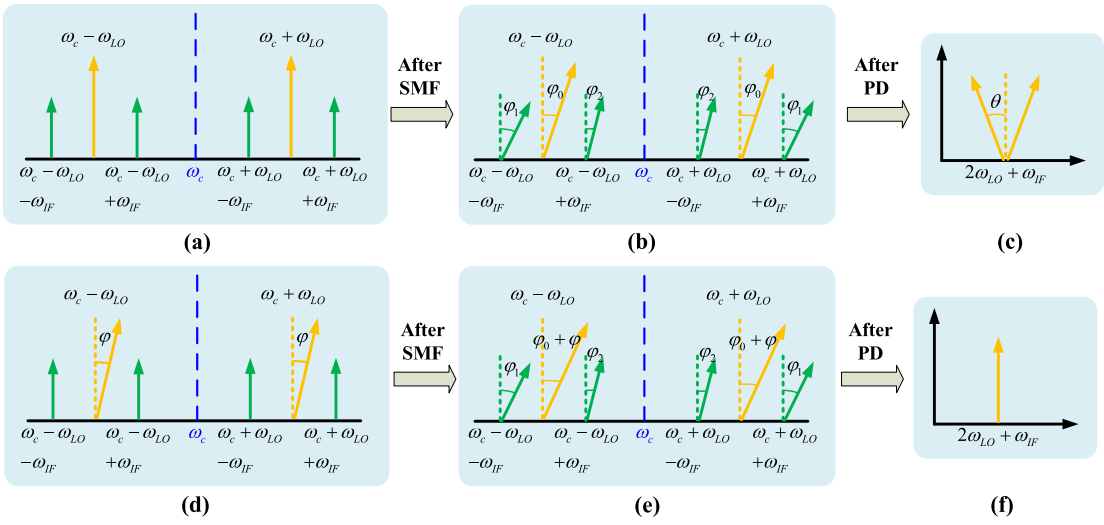

Fig. 3. The spectra analysis of (a), (b), (c) for conventional photonic microwave up-conversion link and (d), (e), (f) for the proposed link. (a), (d) for modulation spectra, (b), (e) for after SMF spectra and (c), (f) for after PD spectra.

3. Simulation Results and Analysis

In order to verify the operational principle of dispersion compensation of proposed technology in Section 2, a proof-of-concept simulation is established using the commercial software VPItransmissionMaker in Fig. 1. In the simulation, a continuous light wave with the frequency of 193.1 THz is injected into the Sagnac loop via an ISO. In the loop, the LO signal with the adjustable frequency of f_{LO} is applied to the PM. Then the output signal of the Sagnac loop is split into two equal optical signals. One part is injected into the MZM which is driven by an IF signal with a signal frequency of f_{IF}. The other part is introduced a phase shift φ. The two parts of the optical signals are combined again and then enter a SMF with length of L, attenuation of 0.2 dB/km, and dispersion parameter of $D = 16\text{ps}/(\text{nm}\cdot\text{km})$. At last, a PD with responsivity of 1 A/W detects the received optical signal. With the use of EDFA, we ensure that the optical signal of about 0 dBm is injected into a wideband PD after the fiber transmission. The EDFA with noise figure of 4 dB is used to compensate the SMF loss and the insertion loss of other devices.

In the proposed link, IF signals at 2.7 GHz and 2.5 GHz are used to transmit over 60 km and 80 km SMFs, respectively. The LO signal is tuned from 4.5 GHz to 11.5 GHz. The frequency responses for the proposed link of 60 km and 80 km are shown in Fig. 4. In the link without compensation, that is, when the phase shift is zero, the RF signal will experience different degrees of power fading. When the fiber length is 60 km and 80 km, the notch points will appear at the frequencies of 24.1 GHz and 19.5 GHz, respectively. At this time, the corresponding LO signal frequencies are 10.7 GHz and 8.5 GHz. In the dispersion compensation link, the phase shift of OPS is adjusted to 60°, 70°, 80° and 90° to compensate the power fading of RF signal which will have different power compensation for different phase shift angles. The difference in the response curves at the four phase shift angles is not obvious, especially near the notch points. However, when the phase shift of the OPS is set at 90°, the maximum power fading points at 24.1 GHz and 19.5 GHz will be best compensated. The power at 24.1 GHz is compensated about 43.08 dB shown in Fig. 4(a). The power at 19.5 GHz is compensated about 43.65 dB shown in Fig. 4(b). By adjusting the φ, the frequency responses can be changed. When φ is set as 90°, the notch points of the grey-blue lines will be shift to the peak points of the red lines.

In the simulation, we sweep the phase shift of the OPS and simulate the power of the desired RF output signal. Fig. 5 shows the relationship of the output RF power and optical phase shift φ at different RF frequencies and fiber lengths. As we can see, when the LO signal frequencies are

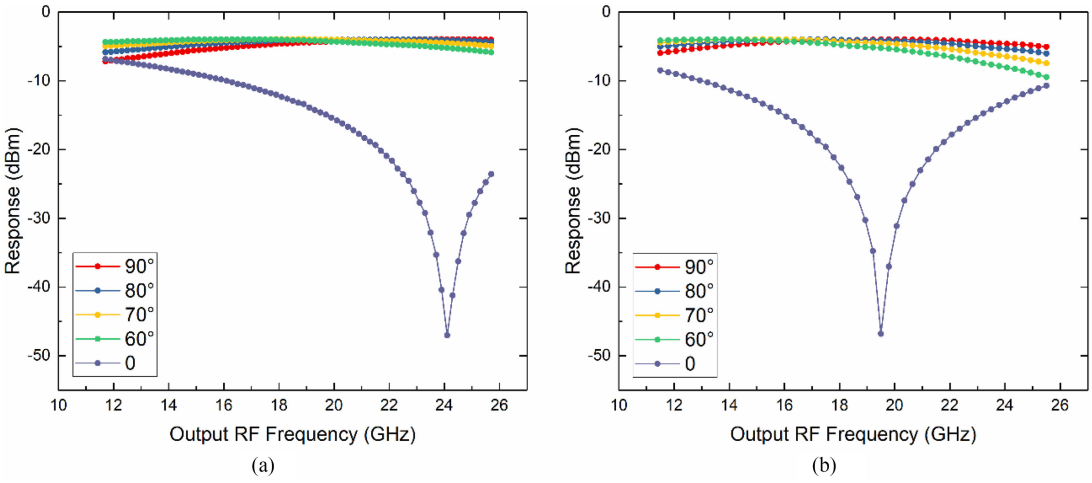

Fig. 4. Frequency responses of the (a) 60 km and (b) 80 km SMFs for different phase shifts. Red lines, for 90° phase shift; Blue lines, for 80° phase shift; Yellow lines, for 70° phase shift; Green lines, for 60° phase shift; Grey-blue lines, for 0 phase shift.

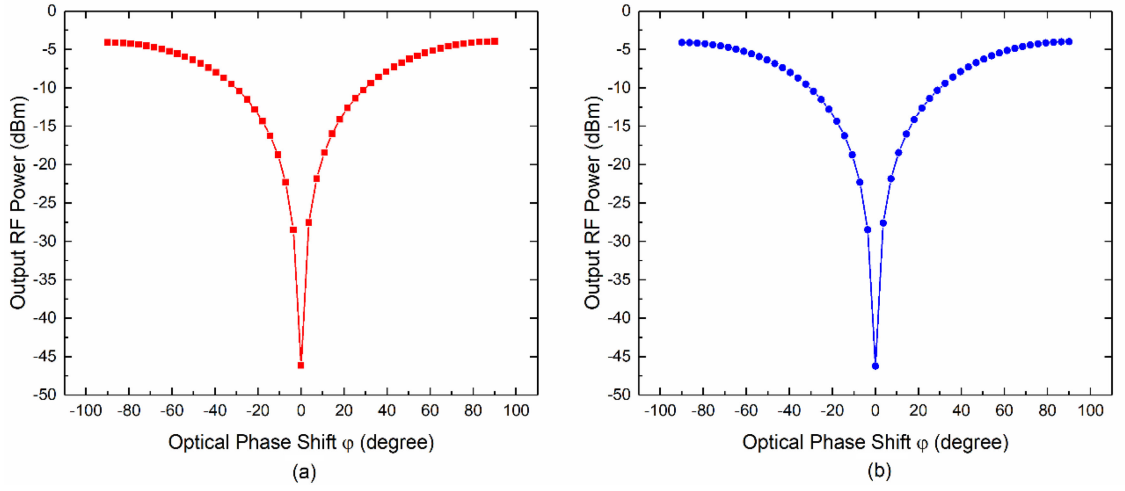

Fig. 5. Simulated output RF power versus optical phase shift [18] for different fiber lengths and frequencies. (a) for 60 km & 24.1 GHz and (b) for 80 km & 19.5 GHz.

fixed at 10.7 GHz and 8.5 GHz, the maximum RF output power are achieved at 90° phase shift after transmitting over 60 km and 80 km SMFs, respectively. Therefore, the corresponding simulation results agree well with equation (14).

Besides, a two-tone IF signal and a LO signal are used to demonstrate the linearity of the proposed up-conversion scheme. The frequencies of the two-tone IF signals are 2.6 GHz and 2.8 GHz while the LO frequency is 10 GHz. At the moment, the corresponding RF signal frequencies are 22.6 GHz and 22.8 GHz, respectively. After the transmission of 60 km SMF, both the power of fundamental signal and third-order inter-modulation distortion (IMD3) signal will have a certain relationship with the input IF signal power. As shown in Fig. 6, the system spurious-free dynamic range (SFDR) is 85.96 dB·$Hz^{2/3}$ at the center frequency of 22.7 GHz with dispersion compensation. Therefore, the SFDR of the proposed link is 13.54 dB higher than that of the link without dispersion compensation.

It is worth noting that the parallel use of MZM and OPS has been mentioned in [19]. MZM is biased at the quadrature transmission point, and effective suppression of IMD3 is achieved by adjusting the

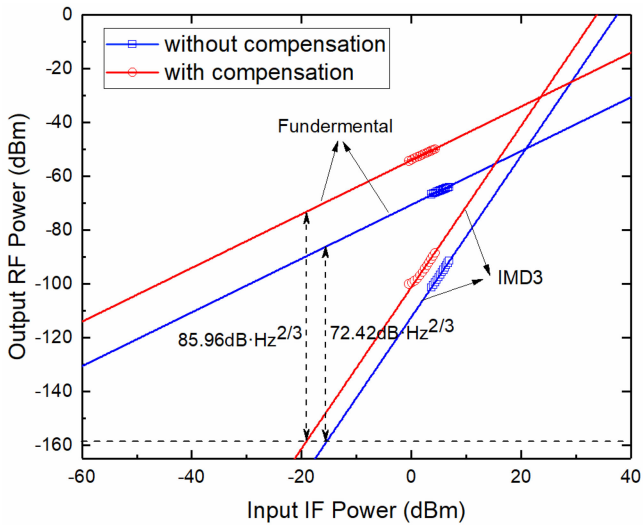

Fig. 6. SFDR results with and without compensation of the proposed links.

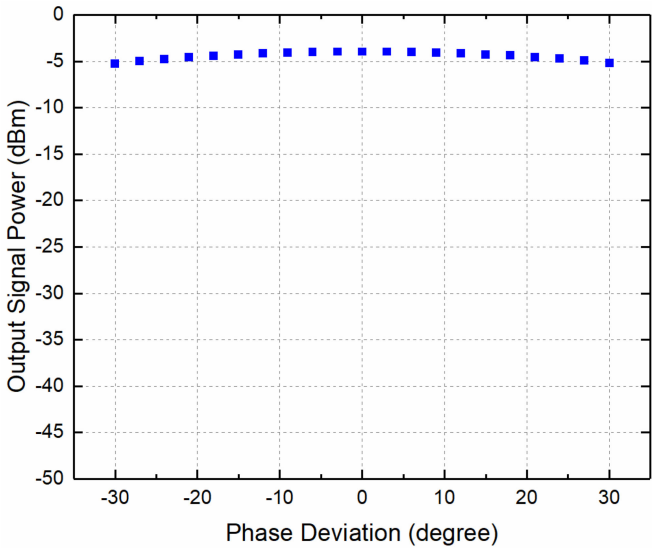

Fig. 7. The desired output signal power versus the phase deviation angle.

phase shift of the OPS and the power split ratio of modulator. However, in the proposed link, MZM is biased at the minimum point to achieve CS-DSB modulation. Then by appropriately adjusting the optical phase shift of the OPS, a high frequency microwave signal with compensation of CDIPF is generated at any frequency.

In the real system, the phase jitter may influence the performance of dispersion compensation. The simulation result of the output signal power versus the phase deviation angle is shown in Fig. 7. The phase deviation angle varies from -30° to 30°.The desired output signal power increases first and then decreases, which is the same as the theoretical analysis. Although the phase deviation angle has reached 30°, the amplitude fluctuation is only 1.26 dB. According to Fig. 7, we can find that the proposed link has a good performance even at inaccurate phase shift angles.

In the above simulation, the output signal of the Sagnac loop is split into two equal optical signals. In order to study the influence of power distribution error on the desired output signal power, the

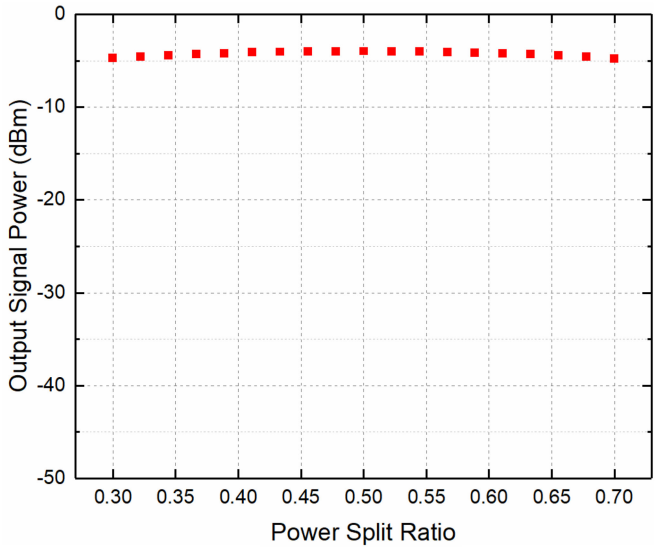

Fig. 8. The desired output signal power versus the power split ratio.

curve of the output signal power versus the power split ratio is shown in Fig. 8. When the power split ratio varies from 0.3 to 0.7, it can be seen from Fig. 8 that the signal power fluctuation is only 0.77 dB. It verifies that a small power split ratio imbalance will not have a significant impact on the output signal power.

4. Conclusion

In this paper, a new photonic frequency up-conversion link is proposed and proved, which is based on the cascading of a Sagnac loop and a MZM. In the Sagnac loop, the PM is bidirectional used because of the inherent characteristics of traveling-wave modulator. The frequency of LO signal is only one-half of the desired RF signal, so the requirements of the LO signal frequency and the PM bandwidth are reduced. In the simulation, power fading of the received RF signal can be successfully compensated and an up-converted RF signal is obtained by adjusting the optical phase shift. In the proposed up-converted link, about 43 dB improvement is demonstrated in frequency response with dispersion compensation. Meanwhile, the SFDR has a 13.54 dB improvement at the certain frequency of 22.7 GHz. Besides, a certain phase deviation angle and a small power split ratio imbalance will not have a significant influence on the output up-converted signal power.

References

[1] J. Yao, "Microwave photonics," *J. Lightw. Technol.*, vol. 27, no. 3, pp. 314–335, 2009.
[2] N. J. Gomes, P. P. Monteiro, and A. Gameiro, *Next Generation Wireless Communications Using Radio Over Fiber*. Hoboken, NJ, USA: Wiley, 2012.
[3] I. Aldaya, J. Beas, G. Castañón, G. Campuzano, and A. Aragón-Zavala, "A survey of key-enabling components for remote millimetric wave generation in radio over fiber networks," *Opt. Laser Technol.*, vol. 49, pp. 213–226, 2013.
[4] V. A. Thomas, M. El-Hajjar, and L. Hanzo, "Millimeter-wave radio over fiber optical upconversion techniques relying on link nonlinearity," *IEEE Commun. Surv. Tut.*, vol. 18, no. 1, pp. 29–53, Jan.–Mar. 2015.
[5] H. Chi and J. Yao, "Frequency quadrupling and upconversion in a radio over fiber link," *J. Lightw. Technol.*, vol. 26, no. 15, pp. 2706–2711, Aug. 2008.
[6] Y. Gao, A. Wen, and H. Zhang, "An efficient photonic mixer with frequency doubling based on a dual-parallel MZM," *Opt. Commun.*, vol. 321, pp. 11–15, 2014.
[7] U. Gliese, S. Norskov, and T. N. Nielsen, "Chromatic dispersion in fiber-optic microwave and millimeter-wave links," *IEEE Trans. Microw. Theory Techn.*, vol. 44, no. 10, pp. 1716–1724, Oct. 1996.
[8] G. H. Smith, A. Nirmalathas, J. Yates, and D. Novak, "Dispersion effects in millimeter-wave fiber-radio systems employing direct-sequence code division multiple access," *Opt. Fiber Technol.*, vol. 5, pp. 165–174, 1999.

[9] Y. Zhang, F. Zhang, and S. Pan, "Optical single sideband modulation with tunable optical carrier-to-sideband ratio," *IEEE Photon. Technol. Lett.*, vol. 26, no. 7, pp. 653–655, Apr. 2014.
[10] W. Zhang, A. Wen, Y. Gao, X. Li, and S. Shang, "Microwave photonic frequency conversion with high conversion efficiency and elimination of dispersion-induced power fading," *IEEE Photon. J.*, vol. 8, no. 3, Jun. 2016, Art. no. 5500909.
[11] G. Yingying *et al.*, "All optical up-converted signal generation with high dispersion tolerance using frequency quadrupling technique for radio over fiber system," *Opt. Laser Technol.*, vol. 79, pp. 153–157, 2016.
[12] C. Yin *et al.*, "Microwave photonic frequency up-convertor with frequency doubling and compensation of chromatic-dispersion-induced power fading," *IEEE Photon. J.*, vol. 9, no. 3, Jun. 2017, Art. no. 5502307.
[13] Y. Gao, A. Wen, L. Liu, S. Tian, S. Xiang, and Y. Wang, "Compensation of the dispersion-induced power fading in an analog photonic link based on PM-IM conversion in a Sagnac loop," *J. Lightw. Technol.*, vol. 33, no. 13, pp. 2899–2904, Jul. 2015.
[14] Y. Gao, A. Wen, X. Wu, Y. Wang, and H. Zhang, "Efficient photonic microwave mixer with compensation of the chromatic dispersion-induced power fading," *J. Lightw. Technol.*, vol. 34, no. 14, pp. 3440–3448, Jul. 2016.
[15] S. Shang, A. Wen, Y. Gao, and W. Zhang, "Tunable frequency-doubled optoelectronic oscillator based on a phase modulator in a Sagnac loop," *Optik Int. J. Light Electron. Opt.*, vol. 145, pp. 617–622, 2017.
[16] A. Altaqui, E. H. W. Chan, and R. A. Minasian, "Wideband microwave photonic downconverters with high dynamic range and high conversion efficiency," in *Proc. IEEE 16th Int. Conf. Transparent Opt. Netw.*, 2014, pp. 1–4.
[17] W. Zhu, M. Zhao, F. Fan, J. Hu, and Y. Gu, "Sagnac interferometer-assisted microwave photonic link with improved dynamic range," *IEEE Photon. J.*, vol. 9, no. 2, Apr. 2017, Art. no. 5500909.
[18] B. Hraimel, X. Zhang, M. Mohamed, and K. Wu, "Precompensated optical double-sideband subcarrier modulation immune to fiber chromatic dispersion-induced radio frequency power fading," *IEEE J. Opt. Commun. Netw.*, vol. 1, no. 4, pp. 331–342, Sep. 2009.
[19] L. Xuan, Z. Shanghong, Z. Zihang, L. Yongjun, Z. Jing, and L. Yun, "Dynamic range improvement of broadband microwave photonic links using a linearized single-sideband modulator," *Opt. Commun.*, vol. 350, pp. 170–177, 2015.